Ma *et al. Chem. Biol. Technol. Agric.* (2024) 11:143
https://doi.org/10.1186/s40538-024-00611-y

Chemical and Biological Technologies in Agriculture

RESEARCH

Open Access

Profiling the lncRNA–miRNA–mRNA interaction network in the cold-resistant exercise period of grape (*Vitis amurensis* Rupr.)

Weifeng Ma[1], Lijuan Ma[2], Zonghuan Ma[1], Wenfang Li[1], Shixiong Lu[1], Huimin Gou[1], Juan Mao[1*] and Baihong Chen[1*]

Abstract

Background Grape is a plant that is sensitive to low temperature and vulnerable to low-temperature damage. However, little is known about the roles of lncRNAs, miRNAs and mRNAs in regulating the hypothermia response mechanism in *Vitis amurensis* Rupr.

Methods In this study, the expression and regulatory network of low-temperature response genes were studied in the phloem of grape under different low-temperature stress.

Results Here, we performed analyses related to RNA-seq and miRNA-seq on grape phloem tissues from five periods of cold resistance campaigns. Three RNAs (lncRNAs, miRNAs and mRNAs) obtained by KEGG and GO analyses were used to identify starch and sucrose metabolism associated with cold resistance, and specific changes in BP, CC, and MF were identified in four comparisons. Venn diagrams, thermograms and pathway maps were used to analyze the differentially expressed genes (DEGs), and their specific gene expression during the cold exercise were obtained. The six DEGs finally selected were used for qRT-PCR to verify the RNA-seq data. In addition, we found that the regulatory networks of miRNAs and lncRNAs correspond to the six DEGs. This study will contribute to further experimental studies to elucidate the cold resistance mechanism of *Vitis amurensis* Rupr.

Conclusions The low-temperature response genes of grape are mainly enriched in the starch and sucrose metabolism, and they are regulated by miRNAs and lncRNAs. The conclusions will provide basic information for further understanding of the cold resistance mechanism of grape in the future.

Keywords Grape, lncRNA–miRNA–mRNA, Low temperature, Full transcriptome analysis, Starch and sucrose metabolism

*Correspondence:
Juan Mao
maojuan@gsau.edu.cn
Baihong Chen
bhch@gsau.edu.cn
Full list of author information is available at the end of the article

Graphical Abstract

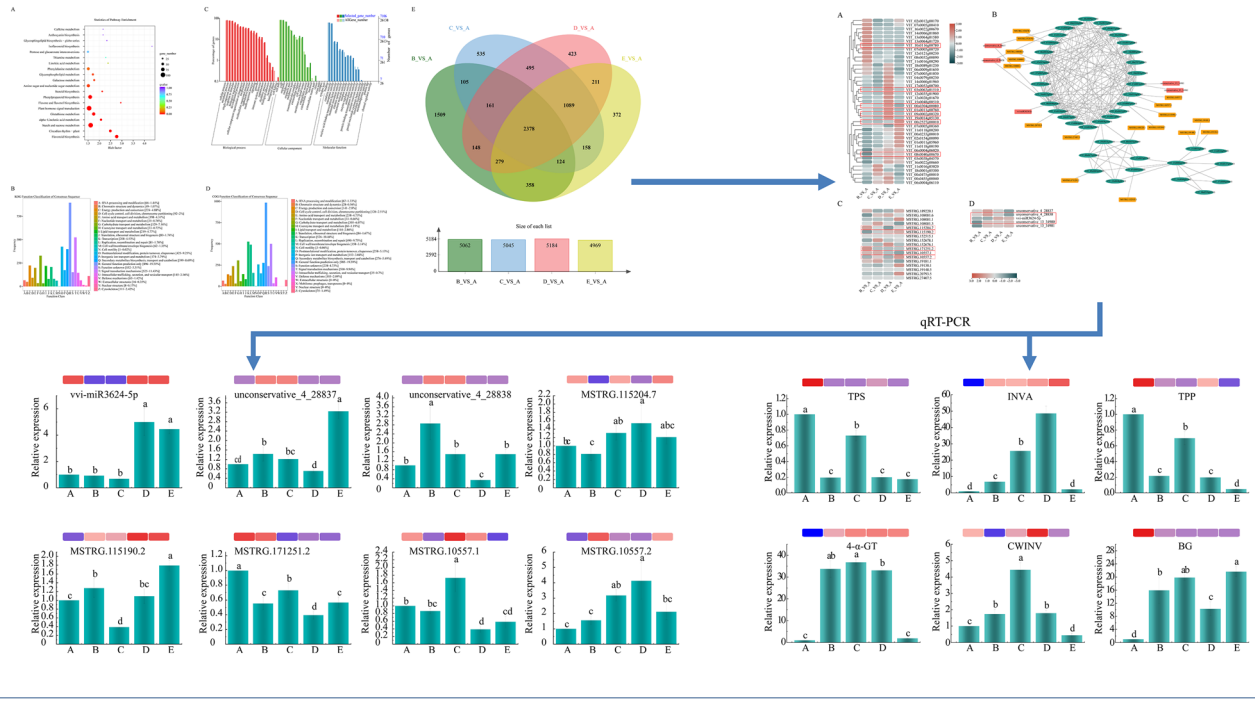

Background

Grapes (*Vitis amurensis* Rupr.), one of the most significant commercial fruit crops, are utilized in various food and beverage businesses, including wine production, raisins, juicing, and fresh cuisine [1]. Low temperature is the most important abiotic stress for normal growth and yield of grapes, and affects the area distribution of grapes [2, 3]. As a result, low temperature is a significant environmental issue that limits the ability of grapes to grow and develop and has an impact on grape output and quality. To enhance grapes' ability to withstand low temperature and make more research on grapes' reaction to low temperature, it is crucial to reveal the molecular mechanism of grape resistance to low temperature.

As deciduous perennials, vines need to be sheltered from freeze before each year's freezing period to survive the winter [4]. Changing gene expression patterns is an efficient and cost-effective strategy to deal with cold stress [5, 6]. Furthermore, numerous cold-responsive genes and the gene products are believed to contribute to cold tolerance at the transcriptional and biochemical levels, as evidenced by earlier research [7–9].

A class of endogenous tiny non-coding RNAs, known as microRNAs (miRNAs), controls the expression of genes [9]. Typically 19–24 nucleotides (nt) long, they originate from stem-loop precursors that are produced by the DICER-LIKE 1 (DCL1) enzyme catalyzing endogenous miR genes [10, 11]. In most eukaryotes, the miRNAs control post-transcriptional gene expression either by facilitating the cleavage of target messenger RNAs (mRNAs) or by suppressing the translation of target mRNAs. This regulation is significant for pathogen response, development regulation, and epigenetic modification [12–16]. Single-stranded RNA molecules are the source of miRNAs [14, 17–19], which imperfectly form secondary structures resembling hairpins locally. Dicer nuclease breaks down these 21 nucleotide molecules from a lengthy RNA precursor with a base pair reentry structure [20]. Base pairing allows the single-stranded version of miRNA to attach to the target RNA by forming a ribonucleoprotein complex with AGO [21, 22]. miRNAs are important post-transcriptional regulators of gene expression. Throughout their life cycle, plants face several abiotic stressors and hormonal cues, to which they might respond in a sequence-specific way. Numerous miRNAs have been found and studied; for example, *miR156* is important in regulating the expression of its target gene, *SPL (PROMOTER BINDING-LIKE)*, which in turn affects plant growth and development [11].

The first miRNA was discovered to regulate development in *C. elegans* in 1993 and it was designated as *Lin-4* [23]. *Ath-miRNA171*, the first plant miRNA, was discovered in 2002 [24]. Recent research on miRNAs has demonstrated the significant function miRNAs play in fruits

such as apple (*Malus domestica*) and grape (*Vitis vinifera*) to response to biotic/abiotic stress [25–27].

Among grapes, 110 miRNAs have been identified [28], including *vvi-miR156a /b/ c* against *Vv-SPL9*, which functions throughout plant growth [11], and *vvimiR061* targets *VvREV* and *VvHOX32*, which play a role in the gibberellin signaling pathway [29]. In addition, miRNAs may regulate certain transcription factors during copper stress, including *AP2*, *SBP*, *NAC*, *MYB* and *ARF* [30].

Although it is known that long non-coding RNAs (lncRNAs) control a wide range of biological activities, what is still unknown is how the entire pool of grape lncRNAs interacts with cold stress. The roles of plant non-coding RNAs, the major types of long non-coding RNAs (lncRNAs) in particular, have not been thoroughly investigated. lncRNA is defined as a non-coding RNA of more than 200 base pairs (bp) in length [31] and it can be divided into four types based on transcript length, including lncRNA, lincRNA (long-intergenic non-coding RNA, large intervening non-coding RNA, long-intervening non-coding RNA), vlincRNA (very long intergenic non-coding RNA), macroRNA and PALR (promoter-associated long RNA) [32]. According to genome-wide analysis, lncRNAs are widely found in plants, including grape [33], *Arabidopsis* [34], rice [35, 36], maize [37], and cotton [38]. The formation of human cancer cells, abiotic and biological stress responses, plant photomorphogenesis, and many other biological processes are affected by the action of lncRNA [39–41]. A previous study found that as a rival for *YUCCA7*, the lncRNA *TCONS_00021861* was demonstrated to suppress *miR528-3p*-mediated cleavage of *YUCCA7* in rice, thus increasing plant tolerance to drought stress [42]. Cotton *lncRNA973* overexpression improves salt tolerance in *Arabidopsis* [43]. lncRNA *asHSFB2a* inhibited the expression of *HSFB2a* in *Arabidopsis*, thus affecting the reaction of plants to heat stress [44]. Similarly, *COLD INDUCED lncRNA 1* (*CIL1*), a novel lncRNA, was found to be a positive regulator of the plant response to cold stress [45]. *LNC_016398-MtCIR1* controls *CBF/DREB1* gene expression in *Medicago truncatula* in response to cold treatment [46]. In grape, lncRNA-mediated regulation of extrachromosomal genes, namely mitochondrial and chloroplast coding sequences, has been observed to be involved in processes such as key biological "photosynthesis" and "oxidative phosphorylation" [33].

Based on full transcriptome data of mRNAs, miRNAs and lncRNAs, we performed four comparisons over five different time periods in this study. The examination of the whole transcriptome data input revealed a high enrichment of mRNAs, miRNAs, and lncRNAs in the starch and sucrose metabolism. Therefore, we carried out an investigation of the interaction networks among mRNAs, lncRNAs, and miRNAs that were enriched in the starch and sucrose metabolism, and some mRNAs were selected for qRT-PCR verification.

Materials and methods

Plant materials and treatments

One-year old grapevine was used in this study, which was developed from the cutting of Chinese wild *Vitis amurensis*. Five different growth stages were selected, including growth stage (A stage, 28 ± 2 ℃, Jul. 9, 2016), earlier low temperature stage (B stage, 5 ± 2 ℃, Oct. 26, 2016), medium low temperature stage (C, 0 ± 2 ℃, Nov. 21, 2016), later low temperature stage (D, − 5 ± 2 ℃, Dec. 28, 2016) and deep dormancy stage (E, − 10 ± 2 ℃, Jan. 9, 2017). The samples were collected from the experiment nursery of Gansu Agricultural University (103° 41′ E, 36° 5′ N). The cultivation substrate includes nearly 30% vermiculite, nearly 40% humus and peat mixed in the proportion of 1:1, and nearly 30% perlite. We selected well-developed trees, cut branches from the ground 40 cm place and quickly brought them to the laboratory. We used garden shears to cut 5–8 cm brachyblast from *Vitis amurensis* branch, and after that, we used the scalpel to remove the cortex and collected the phloem. Three samples collected from each treatment were mixed for transcriptome sequencing. After being gathered, the samples were frozen in liquid nitrogen and kept at − 80 °C.

RNA quantification and qualification

1.5% agarose gels were used to track RNA degradation and contamination, particularly DNA contamination. Thermo Fisher Scientific, Wilmington, DE's Nano Drop 2000 Spectrophotometer was used to quantify the concentration and purity of RNA [47]. With the Agilent Bioanalyzer 2100 System (Agilent Technologies, CA, USA) RNA Nano 6000 Assay Kit, RNA integrity was evaluated [48].

Small RNA library construction

The RNA sample preparation process required 2.5 ng of RNA per sample as input material. With the help of the NEBNext Ultra small RNA Sample Library Prep Kit for Illumina (NEB, USA), and by following the manufacturer's instructions, sequencing libraries were created. Index codes were then applied to each sample to identify its sequences. Ligating the 3′SR Adaptor is the initial step. After mixing RNA, Nuclease-Free Water, and 3'SR Adaptor, the mixture was heated to 70 ℃ for two minutes and then put in the ice. Next, 3′ Ligation Enzyme and 3′ Ligation Reaction Buffer (2X) were added to create the combination and the heat cycler was set to 25 ℃ for an hour to attach the 3'SR Adaptor. After the 3' binding

procedure, the excess 3'SR adaptors that are still free are hybridized with SR RT primers to stop dimer adaptor formation, which then transformed single-stranded DNA (ssDNA) adaptors into double-stranded DNA (dsDNA) molecules (dsDNA is not a ligation-mediated substrate). The 5′SR Adaptor must be ligated in the second step. And the first chain was synthesized through reverse transcription. The last step includes PCR amplification and Size Selection. PAGE gel was used for electrophoresis and the fragment were sorted to form a small RNA library. Agilent Bioanalyzer 2100 system [48] was used to evaluate the library quality after PCR products were purified by using the AMPure XP system [49].

lncRNA and mRNA library construction

The Ribo-Zero rRNA Removal Kit (Epicenter, Madison, WI, USA) was used to extract rRNA from the samples by using 1.5 μg of RNA per sample. The NEBNextR UltraTM Directional RNA Library Prep Kit for IlluminaR (NEB, USA) was used to produce sequencing libraries in accordance with the manufacturer's instructions. Index codes were incorporated to assign sequences to individual samples. Divalent cations were used in NEBNext First Strand Synthesis Reaction Buffer (5X) at a high temperature to carry out the fragmentation process. Random hexamer primer and reverse transcriptase were used to create first strand cDNA. Next, RNase H and DNA Polymerase I were used to synthesize second-strand cDNA molecules. Through the use of exonuclease and polymerase, the remaining overhangs were transformed into blunt ends. To get ready for hybridization, the 3' ends of DNA fragments were adenylated, and then the NEBNext Adaptor with a hairpin loop structure was ligated. AMPure XP Beads (Beckman Coulter, Beverly, USA) were used to purify the library fragments in order to choose pieces with the ideal length of 150–200 bp [49]. Next, selector-ligated cDNA was treated with 3 μl USER Enzyme (NEB, USA) at 37 °C for 15 min before PCR. Then, Phusion High-Fidelity DNA polymerase, Universal PCR primers, and Index(X) primer were used to carry out PCR. Finally, the AMPure XP system [49] was used to purify the PCR products, and qPCR and the Agilent Bioanalyzer 2100 [48] were used to evaluate the library quality.

Clustering and sequencing

By following the manufacturer's instructions, the index-coded samples were clustered by using a cBot Cluster Generation System and the TruSeq PE Cluster Kit v4-cBot-HS (Illumina) [50]. After the cluster creation, paired-end reads were produced and the library preparations were sequenced on an Illumina Hiseq 2500 platform [51].

Sequence analysis results of microRNA: mapping and differential expression

Initially, internal Perl scripts were used to process the raw data (raw readings) in the Fastq format. In this stage, low-quality reads, adapter-containing reads, and ploy-N-containing reads were eliminated from the raw data to get clean data (clean reads). Next, sequences longer than 30 nt or less than 18 nt were removed from the readings in order to trim and clean them. Concurrently, the clean data's Q20, Q30, GC-content, and sequence duplication level were determined. The clear, high-quality data served as the foundation for all downstream studies.

By using the Bowtie Tools software [52], Ribosomal RNA (rRNA), small nuclear RNA (snRNA), small nucleolar RNA (snoRNA), small nucleosomal RNA (snoRNA), transfer RNA (tRNA), other non-coding RNAs, and some repeats were filtered by using clean reads that were sequenced against the GtRNAdb, Silva, Repbase, and Rfam databases, respectively. By comparing the remaining reads with known miRNAs from miRbase (https://www.mirbase.org/), it was possible to identify the known miRNAs and the novel miRNAs predicted. The prediction of new miRNA secondary structures was done by using Randfold. [53]. For every sample, the levels of miRNA expression were estimated: 1. The precursor sequence was mapped back to the sRNAs; 2. The mapping findings were used to determine the read count of each miRNA.

Prior to performing DEGs analysis, each sequenced library's two treatments were subjected to a differential expression analysis by using IDEG6 for samples lacking biological duplicates. The criterion for significantly differential expression was established at qvalue < 0.05 & |log2 (foldchange) | ≥ 2 [54].

Sequence analysis results of lncRNA and mRNA: mapping and differential expression

Initially, internal Perl scripts were used to process the raw data (raw readings) in the Fastq format. In this stage, low-quality reads, adapter-containing reads, and ploy-N-containing reads were eliminated from the raw data to get clean data (clean reads). Next, sequences longer than 30 nt or less than 18 nt were removed from the readings in order to trim and clean them. Concurrently, the clean data's Q20, Q30, GC-content, and sequence duplication level were determined. The clear, high-quality data served as the foundation for all downstream studies.

Based on the sequences mapped to the reference genome, the transcriptome was constructed by using StringTie [55]. The collected transcripts were annotated in the gffcompare software. To find potential lncRNAs, the unidentified transcripts were screened. The transcriptome was assembled by using the StringTie based

on the reads mapped to the reference genome. The gffcompare program was used to annotate the assembled transcripts. The unknown transcripts were used to screen for putative lncRNAs. In order to separate potential protein-coding RNAs from non-protein-coding RNA candidates in the unidentified transcripts, four computational techniques—CPC/CNCI/Pfam/CPAT—were combined. Potential RNAs that code for proteins were eliminated based on a cutoff point for exon number and minimum length. As lncRNAs candidates, transcripts longer than 200 nt and including more than two exons were chosen. These transcripts were then screened by using CPC/CNCI/Pfam/CPAT, which can differentiate between genes that code for proteins and those that do not. Additionally, the various kinds of lncRNA—lincRNA, intronic lncRNA, anti-sense lncRNA, and sense lncRNA—were chosen through the application of cuffcompare.

The FPKMs of the coding genes and lncRNAs in each sample were determined by using StringTie (1.3.1) [56]. The FPKMs of transcripts in each gene group were added up to calculate the gene FPKMs. Based on the length of the fragment and the number of reads mapped to it, FPKM stands for fragment per kilo-base of exon per million fragments mapped.

Before performing a differential gene expression analysis on samples without biological replicates, the edgeR computer package corrected the read counts for each sequenced library by using a single scaling normalization factor. Two samples were subjected to differential expression analysis by using the EBseq (2010) R program. The posterior probability of being DE, or PPDE, was used to modify the resulting FDR (false discovery rate). The criterion for significantly differential expression was set at FDR < 0.05 & |log2 (fold change) | ≥ 2.

Functional analysis of DEGs

To determine which DEGs were significantly enriched in GO keywords or metabolic pathways, functional enrichment analysis by using KEGG and GO was carried out. By utilizing the Wallenius non-central hyper-geometric distribution based on GO seq R tools, GO enrichment analysis of the DEGs was carried out [57]. Specifically, large-scale molecular datasets produced by genome sequencing and other high-throughput experimental technologies are the main source of information for KEGG, a database resource for understanding high-level functions and utilities of the biological system, such as the cell, the organism, and the ecosystem (http://www.genome.jp/kegg/) [58]. We tested the statistical enrichment of differential expression genes in KEGG pathways by using the KOBAS [59] software.

Quantitative real-time PCR validation of RNA-seq data

In order to verify the expression of mRNA grape phloem samples in five stages of A, B, C, D, and E, the RNA returned by the sequencing company was reversely transcribed into cDNA by using TaKaRa (Dalian, China) PrimeScriptTMRT Reagent Kit (Perfect Real Time). The cDNA was then adopted for q-PCR experiments with the help of a Bio-Rad iCycler iQ real-time quantitative PCR instrument and SYBR Primer Ex TaqTM II reagent. Sangon Biotech designed and synthesized the primers for qRT-PCR. The first cDNA strand of miRNA was synthesized by tail addition method, and the 3 'primer was synthesized by Accurate Biotechnology (Hunan) Co., Ltd. *VvGAPDH* (NCBI reference sequence ID: XM_0022663109) was used as an internal control gene for mRNA and lncRNA expression standardization. And *VvU6* was used as an internal control gene for miRNA expression standardization. The primers used are shown in the following Supplementary Table 1.

Statistical analysis

Excel 2010 was used to analyze the transcriptome data and qRT-PCR results. Differences among means were evaluated by the least-significant difference (LSD) with the Statistical Program for Social Science 19 (SPSS, Chicago, IL, USA). Graphs were generated with Origin 9.0.

Results

Illumina sequencing

To reveal the mechanism of the response to low-temperature stress in *Vitis amurensis* Rupr., the whole transcriptome sequencing was performed on phloems of different low-temperature periods and the transcripts were compared. Low-quality data were removed and quality analysis can be found in Supplementary Table 2. The total reads of mRNA with lncRNA for the five samples of A, B, C, D and E with different low-temperature exercise periods were 127.6, 132.4, 110.7, 108.7, 108.8, respectively. And the total reads of miRNA for the five samples were 5.3, 11.5, 2.7, 9.5, 9.8 million, respectively. The total reads of mRNA plus lncRNA were much higher than those of miRNA. The Mapped Reads of mRNA and lncRNA in 5 samples were 56.17% at the lowest and 75.79% at the highest. And the Mapped Reads of miRNA were all above 34%, with the lowest being 34.16% and the highest being 43.24%. Uniq Mapped Reads of each sample mRNA and lncRNA were above 50%, and the highest was sample B, reaching 74.07%. The Multiple Mapped Reads of each sample were low, ranging from 1.34% to 1.80%. In addition, the Reads Map to '+' of each sample was higher than that to '−', the Reads Map to '+' was higher than 20%, and the Reads Map to '−' was higher than 12%. The GC content ranged from 46.44% to 52.55 and the Q30

was above 95% in all samples. It can be seen that the transcripts are of good quality and can be used for subsequent analysis.

Global gene analysis

Gene expression analysis of each comparison group revealed that more than half of the gene expressions were upregulated in each low-temperature treated sample compared to those in the growth stage (A), with C VS A, D VS A and E VS A upregulating almost three times more genes than down-regulating genes (Fig. 1A). In addition, with the deepening of low-temperature, the number of DEGs in D period was the highest (5175), with 3686 upregulated genes and 1498 down-regulated genes. It can be seen that after the low-temperature treatment, most genes were upregulated in expression when in response to low-temperature stress. Different from mRNAs, with the deepening of low-temperature stress, the number of upregulated miRNAs of B VS A was 1.67 times that of down-regulated gene, and the number of upregulated genes of C VS A, D VS A and E VS A were 0.78 times, 0.69 times and 0.975 times that of down-regulated gene, respectively. These indicate a decrease in the number of upregulated miRNAs. The changing trend of mRNA gene expression was opposite (Fig. 1B). The number of differential lncRNAs decreased sharply in C VS A, and the number of upregulated lncRNAs was lower than that of down-regulated lncRNAs. After the intensification of low-temperature stress, the number of differential lncRNAs gradually increased, and the number of upregulated lncRNAs was higher than that of down-regulated lncRNAs in D VS A and E VS A, respectively (Fig. 1C).

The assembled data were analyzed against major databases by using BLAST software to obtain annotation information for all genes. A total of 20,260 genes were annotated in the given protein database search. The NR database had the most annotated genes (20,258), the GO and Swiss-Prot databases also had more than 10,000 annotated genes (17,243 and 15,186, respectively), while the KEGG database had the least annotated genes (6062) (Fig. 1D). Similar to mRNAs, miRNAs and lncRNAs had the most annotations in the RN database, with 7567 and 15,066, respectively. The numbers of their genes annotated in GO database ranked the second, 7267 and 13,397, respectively, while the numbers of their genes annotated in KEGG database were the least, 2897 and 5516, respectively (Fig. 1E, F).

Differential gene enrichment analysis

DEGs enrichment analysis showed that in the KEGG database, alpha-linolenic acid metabolism, flavonoid biosynthesis, circadian rhythm plant, starch and sucrose metabolism, and alpha-linolenic acid metabolism were the primary areas in which DEGs were abundant (Fig. 2A). Proteins inferred from the identified RNA sequences were mapped and grouped into 24 functional

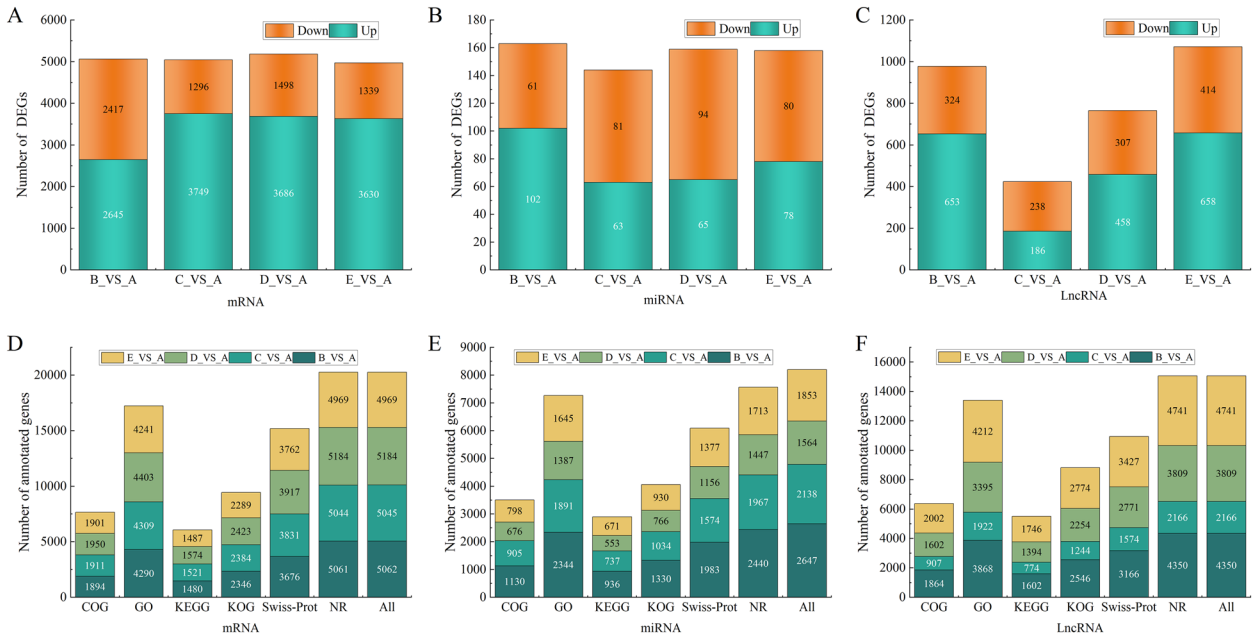

Fig. 1 The number of DEGs was compared with the annotation library. Number of mRNAs, miRNAs and lncRNAs up- and down-regulated at different low-temperature comparisons, **A** mRNA, **B** miRNA, **C** lncRNA. Basic local alignment search tool (BLAST) was used to compare nucleic acid sequence to protein sequence library (BLASTx) against specific platforms, **D** mRNA, **E** miRNA, **F** lncRNA

classes in KOG database, mostly annotated in the areas of chaperones, protein turnover, signal transduction processes, carbohydrate transport and metabolism, post-translational modification, and the formation, transport, and catabolism of secondary metabolites (Fig. 2B). DEGs were classified into 55 functional groups by the GO database, which were divided into 3 subclasses, including biological processes, cell components, and molecular functions (Fig. 2C). In the COG database, DEGs were annotated and grouped into 23 categories, of which cell motility was the least annotated (Fig. 2D).

Venn analysis of B_VS_A, C_VS_A, D_VS_A and E_VS_A revealed that 2,378 genes co-occurred in the four treatment groups, showing that all 2,378 genes were differentially expressed with increasing levels of stress. Subsequent analyses are carried out on these 2,378 genes (Fig. 2E).

GO enrichment analysis was performed on 2,378 genes in B_VS_A, C_VS_A, D_VS_A and E_VS_A. It was found that Biological process, cellular component and molecular function contained 19, 14 and 14 functional groups, respectively (Fig. 3A). In addition, the frequency of upregulated genes in biological processes, cell components and molecular functions reached 17,930, the frequency of down-regulated genes was 5,650, and the frequency of upregulated genes was three times that of down-regulated genes. Further analysis showed that GO: 0016530 and GO: 0045735 were both upregulated genes in molecular function.

Meanwhile, KEGG enrichment of 2378 common DEGs showed that the DEGs were mainly in pentose and glucuronate interconversions, alpha-linolenic acid metabolism, flavone and flavonol biosynthesis, Starch and sucrose metabolism, flavonoid biosynthesis and circadian rhythm-plant (Fig. 3B). After that, the target genes of differentially expressed miRNAs and lncRNAs were analyzed by KEGG classification (Fig. 4A, B). And it was found that their target genes were classified into five categories: metabolism, organismal systems, genetic information processing, environmental information processing, and cellular processes. The distinction is that in the context of environmental information processing, ABC transporters, phosphatidylinositol signaling system, and plant hormone signal transduction were the target genes of miRNAs. Conversely, the annotation of lncRNA target genes was limited to the plant hormone signal transduction pathway. In genetic information processing, miRNAs were not annotated to the SNARE interactions in vesicular transport pathway, and lncRNAs are not annotated to the aminoacyl-tRNA biosynthesis pathway. In metabolism, the target gene annotations of miRNAs and lncRNAs varied greatly, but both of them were annotated in the carbon metabolism and starch and sucrose metabolism. Taken together, the significant enrichment of mRNAs and the target genes of miRNAs and lncRNAs in the starch and sucrose metabolism suggest that genes associated with the starch and sucrose metabolism may respond to low-temperature stress. Therefore,

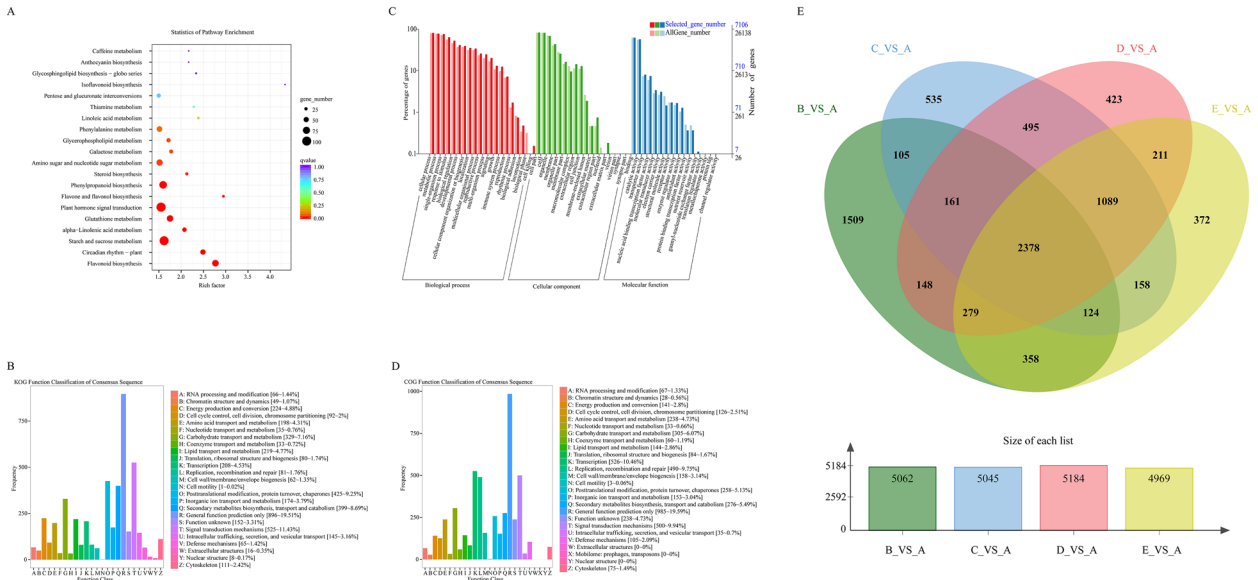

Fig. 2 Annotation of differentially expressed genes (DEGs) in different databases and differential Venn plots. **A** KEGG database enrichment plot. **B** KOG database enrichment plot. **C** GO database enrichment plot. **D** COG database enrichment plot. **E** Top half, Venn diagram between different treatments. In the second part, the number of different genes differs between different treatments

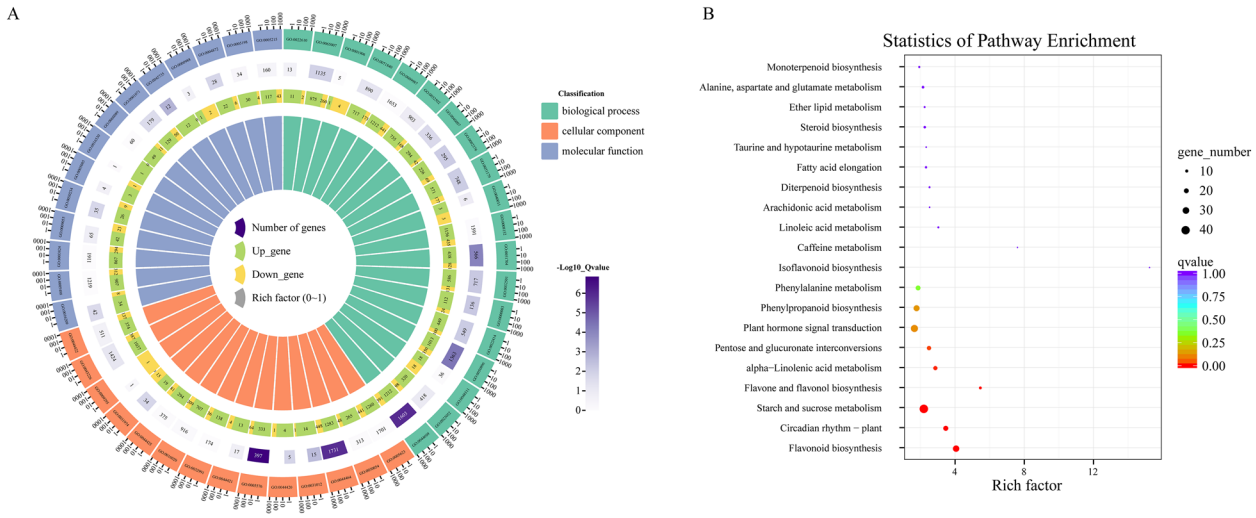

Fig. 3 Annotation of differential DEGs in different databases. **A** GO database enrichment diagram. Outermost layer, the GO term; Second, the number of genes enriched by the GO item; In the third layer, the number of upregulated (yellow-green) genes and down-regulated (yellow) genes. **B** KEGG database enrichment map. The size of the bubble represents the number of genes, and the larger the bubble, the more genes

Fig. 4 miRNA and lncRNA target gene KEGG annotation. **A** miRNA target gene KEGG annotation. **B** lncRNA target gene KEGG annotation

subsequent analyses focus on the starch and sucrose metabolism.

mRNA, miRNA and lncRNA length analysis

As shown in Fig. 5A, the length of mRNAs was above 200 nt, and the number of mRNAs of 200 nt in length was 1358, which is less than that of mRNAs of 3000 nt in length; the number of mRNAs of 400 nt in length was the highest, with 103,766, and among those with the length of over 400 nt, the longer, the fewer; the total number of mRNAs of over 3000 nt in length was 26,315, which is lower than the number of mRNAs of 600 nt in length. The length of lncRNAs was over 400 nt, and the number of lncRNA fragments with the length of 400 nt was the highest, which was 4669. As the length of lncRNA fragments increased, the number of lncRNAs longer than 400 nt decreased; there are 129 lncRNAs totaling 3200 nt in length (Fig. 5B).

The length of the miRNAs varied from 18 to 24 nt, with 104 with the length of 21 nt, which is the most common length. And there were 75 miRNAs with a length of 24 nt, making it the second most common kind. The fewest miRNAs among them are those with the length of 18 or 19 nt, only 4 in total (Fig. 5C).

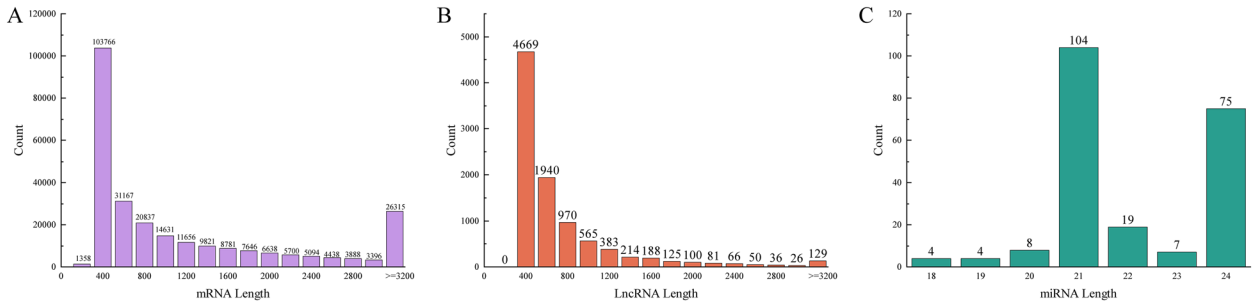

Fig. 5 The lengths of the three RNAs. **A** mRNA length. **B** lncRNA length. **C** miRNA length. The horizontal axis represents the length of the gene, and the vertical axis represents the number of genes

Correlation analysis of mRNA with miRNA and lncRNA based on FPKM value

Correlation analysis was performed on the FPKM values with 41 mRNAs, 5 miRNAs and 17 lncRNAs. As is shown in Fig. 6, *unconservative_4_28837*, *unconservative_4_28838*, *unconservative_13_34980* and *unconservative_13_34981* were positively correlated with 29 mRNAs. The correlation patterns were similar, but *nconservative_4_28837* and *unconservative_4_28838* had stronger correlation with 29 genes. While vvi_miR3624_5p was positively correlated with only 10 mRNAs. In addition, *MSTRG.108081.3*, *MS TRG.152515.1*, *MSTRG.10557.2*, *MSTRG.19181.1*, *MSTRG.19130.1*, *MSTRG.19148.5*, and *MSTRG.20793.5* were positively correlated with most of the genes in the starch and sucrose metabolism, and *MSTRG.108081.3*, *MS TRG.152515.1*, *MSTRG.10557.2* and *MSTRG.19181.1* showed similar patterns of correlation.

Analysis of mRNA interactions with miRNA and lncRNA

To explore the expression of mRNAs in the starch and sucrose metabolism and the interactions network relationship among mRNAs, miRNAs and lncRNAs, we drew a heatmap of miRNA expression based on the FPKM values and visualized the interaction network among mRNAs, miRNAs and lncRNAs.

In Fig. 7A, heatmaps were drawn for the FPKM values of 41 genes enriched in the starch and sucrose metabolism. *TPP* (trehalose 6-phosphate phosphatase), *CWINV* (Cell wall invertase), and *TPS* (alpha,alpha-trehalose-phosphate synthase) were upregulated in D and down-regulated in B, C, and E, *INVA* (invertase) was upregulated in E and *4-α-GT* (4-alpha-glucanotransferase) is upregulated in C, D, and E, compared with that in A.

To clarify the interactions of mRNAs, miRNAs and lncRNAs, the interaction network was visualized by Cytoscape (Fig. 7B, Supplementary Table 3). *VIT_17s0053g00700* was found to be regulated by two miRNAs, *unconservative_13_34981* and *unconservative_13_34980*. The expression of *TPP* and *4-α-GT* were regulated by *unconservative_4_28837* and *unconservative_4_28838*, and the expression of *4-α-GT* was also regulated by *vvi-miR3624-5p*. In addition, the expression of *VIT_02s0154g00090* was regulated by three lncRNAs, namely *MSTRG.108081.6*, *MSTRG.108081.3* and *MSTRG.108081.1*, and the expression of *VIT_11s0016g03020* was regulated by *MSTRG.19181.1*, *MSTRG.19130.1* and *MSTRG.19148.5*. The expression of *VIT_07s0005g01030* was regulated by *MSTRG.152678.1* and *MSTRG.152676.1*, the expression of *BG* (beta-glucosidase) was regulated by *MSTRG.10557.2* and *MSTRG.10557.1*, and the expression of *VIT 03s0063g01510* was regulated by *MSRG.11516.1000101016*. After that, based on the interaction genes that regulate low-temperature stress and have different correlation types with miRNAs and lncRNAs, 6 mRNAs were selected for further analysis, and 1 interacted with 3 miRNAs, 1 interacted with 2 miRNAs, 1 interacted with 2 lncRNAs, 1 interacted with 1 lncRNA, 1 interacted with 1 mRNA, and 1 did not interacted any miRNA or lncRNA (Fig. 7A). Meanwhile, miRNAs (*unconservative_4_28838*, *vvi-miR3624-5p*, *unconservative_13_34980*) and lncRNAs (*MSTRG.115204.7*, *MSTRG.115190.2*, *MSTRG.171251.2*, *MSTRG.10557.1*, *MSTRG.10557.2*) that interacted with candidate mRNAs and had inconsistent expression patterns were selected for further analysis (Fig. 7C, D).

Transcriptome data qRT-PCR validation

In order to verify the results of RNA-seq, we performed qRT-PCR verification, and selected 6 differentially expressed mRNAs in the starch and sucrose metabolism. Additionally, five lncRNAs and three miRNAs that interact with the six genes mentioned above but have different expression patterns were chosen for qRT-PCR. For every gene, three biological replicates were carried out, and the

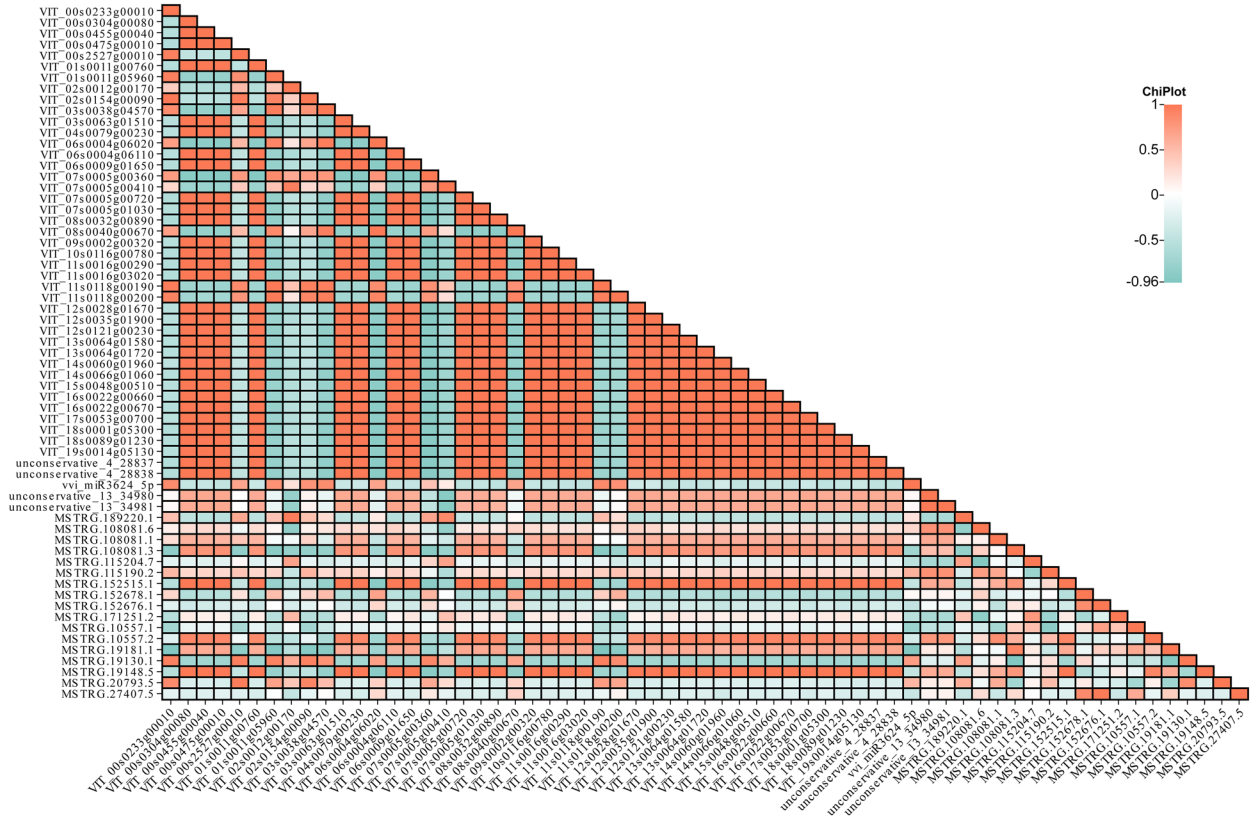

Fig. 6 Correlation analysis of mRNA, miRNA and lncRNA based on FPKM values

relationship between the RNA-seq and qRT-PCR data was examined. The results are shown in Fig. 8.

The expressions of *TPS* and *TPP* were down-regulated under the condition of deepening low temperature, and only upregulated briefly in period C. The expressions of *INVA* and *BG* increased with the intensification of low temperature, but *INVA* decreased in E period. *4-a-GT* and *CWINV* had similar expression patterns, both of which were significantly upregulated at B, C and D stages, and reached the peak expression at C stage. The relative expression level of *vvi-miR3624-5p* significantly increased in D and E period, and the relative expression level of *MSTRG.115204.7* significantly increased in D period. The relative expression of *unconservative_4_28837* dramatically increased in E period, and the expression of *unconservative_4_28838* significantly increased in B period. The relative expression level of *MSTRG.115190.2* increased with the deepening of low temperature except in the C period, while the expression trend of *MSTRG.171251.2* and *MSTRG.10557.1* was opposite to that of *MSTRG.115190.2*. The relative expression of *MSTRG.10557.2* increased gradually with the intensification of low temperature, and decreased dramatically in E period.

Both *BG* and *vvi-miR3624-5p* showed differences in transcriptome sequence data at stage A, *unconservative_4_28837* showed differences in transcriptome sequencing data at stage E, and *MSTRG.10557.2* showed differences in transcriptome sequencing data at stage B. The remaining genes showed consistent expression trends in RNA-seq and RT-qPCR at all stages, indicating that there was the consistency between transcript abundance determined by RNA-seq and data obtained from RT-qPCR.

Discussion

Based on the sequencing quality of the whole transcriptome data (as shown in Supplementary Table 2), it can be seen that the sequencing quality is good enough to be used for later data analysis. Among all types of RNA distributions, mRNAs were the most, followed by lncRNAs, and miRNAs were the least. From the overall distribution of three expression levels, it is concluded that the five samples have a high degree of coincidence, and their peaks are basically the same. After identifying the length distributions of lncRNAs, mRNAs and miRNAs, we have found that the length of lncRNAs and mRNAs is over 200 nt, and that the length of miRNAs is mainly concentrated

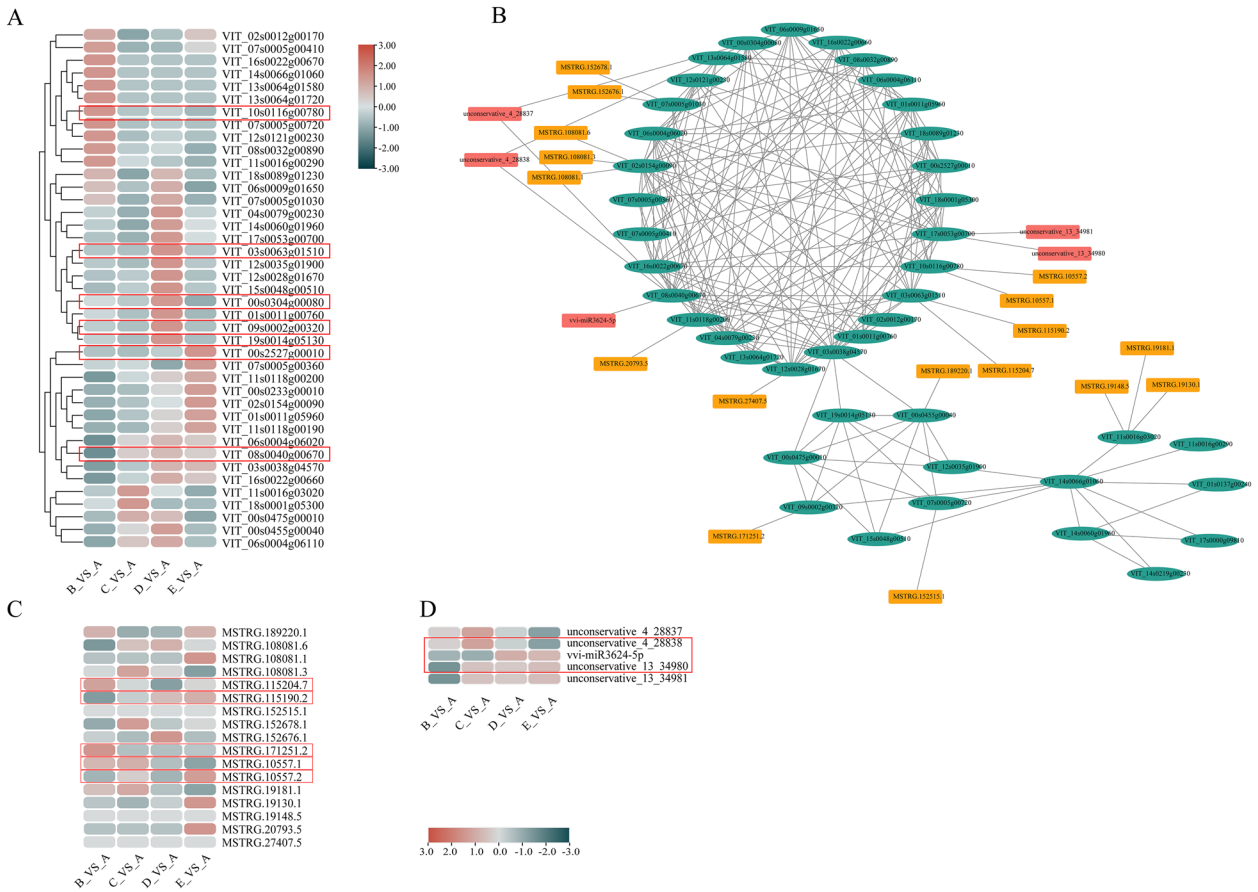

Fig. 7 Heat map of expression genes and regulatory network of related genes with miRNAs and lncRNAs in starch and sucrose metabolism (**A** mRNA, **C** lncRNA, **D** miRNA). Differential expression levels are based on the fragments per kilobase of transcript per million fragments (FPKM) values. The FPKM values of genes were transformed by log2. **B** Network diagram of mRNA interactions with miRNA and lncRNA

at 21nt, followed by 24 nt. Due to the specificity of Dicer and DCL enzymes, the length of mature miRNAs mainly ranges from 20 to 24 nt. Among animals, the length of miRNAs is mainly 22 nt, but for plans, 21 nt or 24 nt is the most common length of miRNAs [60].

With the help of KEGG enrichment analysis, the expansion analysis was effectively carried out on a specific pathway. *DEGs* can be identified throughout the pathway, and upstream and downstream relationship nodes can be obtained [61]. Numerous DEGs were considerably enriched in the production of flavones and flavonols, as well as in the starch and sucrose metabolism, according to KEGG expression analysis. Both miRNAs and lncRNAs have target genes that are abundant in the starch and sucrose metabolism, according to the KEGG classification of those genes. It can be seen that genes related to starch and sucrose metabolism significantly respond to low-temperature stimulation under low-temperature exercise. GO Database established by GO Organization (Gene Ontology Consortium) is a structured standard biological annotation system, built in 2000. The purpose is to establish a standard vocabulary system of product knowledge and its genes, which is applicable in various species [62]. In this paper, GO analysis of DEGs showed that a large amount of DEGs was enriched in the molecular functional module, and a small amount of DEGs was distributed in the cellular component module. The results showed that the molecular function played a significant role under low-temperature stimulation.

The primary glucose-related pathways found in KEGG are those linked to the starch and sucrose metabolism, fructose and mannose, galactose, glycosaminoglycan degradation of pentose and glucuronic acid interconversion, and glycans. Although the target gene annotation pathways of lncRNAs and miRNAs were different, they were both annotated in the starch and sucrose metabolism. Coincidentally, mRNA is also significantly enriched in the starch and sucrose metabolism.

The starch and sucrose metabolism were selected, and the differentially expressed mRNAs were analyzed by

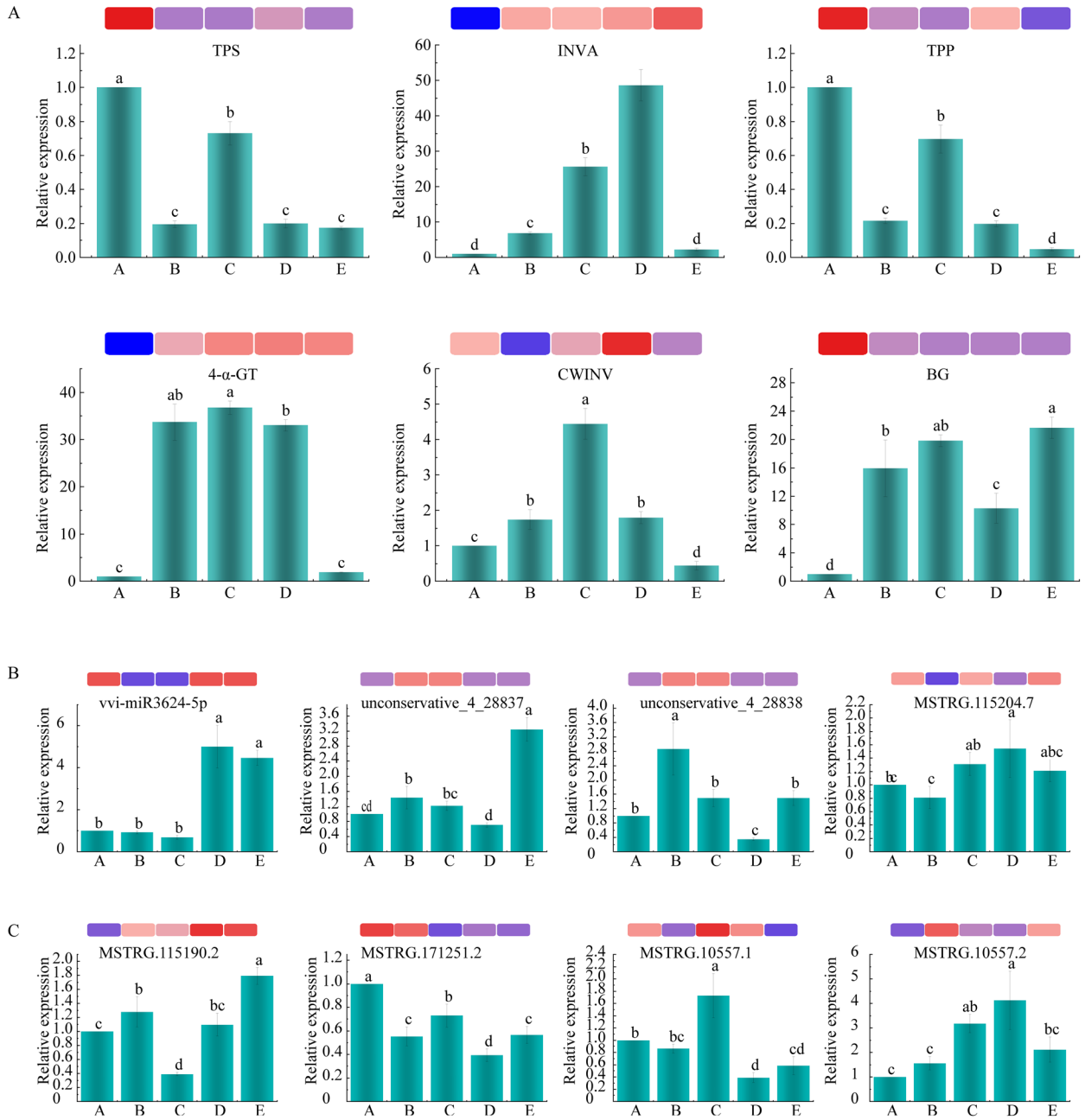

Fig. 8 qRT-PCR verifies transcriptome data of mRNA, miRNA and lncRNA. **A** q-RTPCR results of mRNA, **B** q-RTPCR results of miRNA, and **C** q-RTPCR results of lncRNA. The heat map above the graph of relative expression quantity of each gene shows the FPKM value of the gene. The redder the color, the larger the FPKM value, and the bluer the color, the smaller the FPKM value

heatmap, and the interactions among mRNAs, miRNAs and lncRNAs were mapped. Six differentially expressed mRNAs in the pathway that were positively regulated by miRNAs and lncRNAs were used for further analysis. There were only seven miRNAs that regulate mRNAs, most of which were unknown miRNAs, and the only known miRNA was *vvi-miR3624-5p*. Previous studies have found that *vvi-miR3624* can be induced by cold stress, and its expression tends to increase when treated at low temperatures [63]. The study confirmed that *Metal Ion Binding Protein* mRNA is the target of *miR3624-3p* [25, 63]. Nevertheless, the lack of related reports in other species suggests that miR3624 is unique to Vitis. Moreover, the regulatory link between miRNA and mRNA is

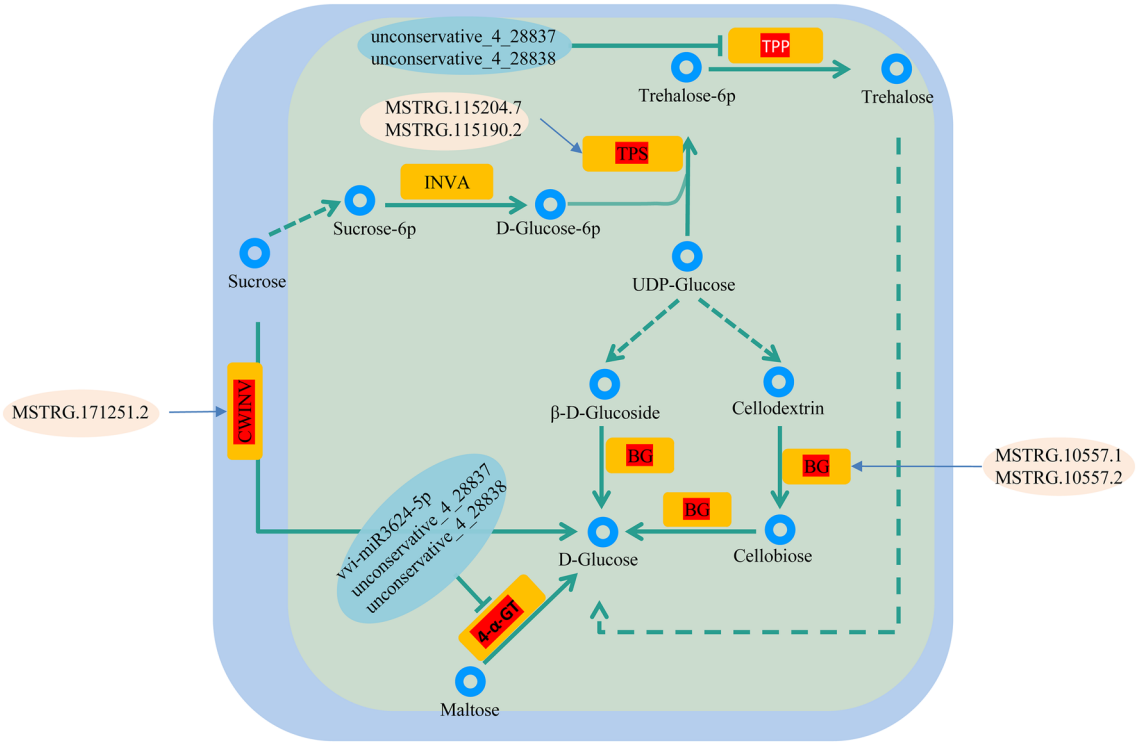

Fig. 9 Hypothetical model of mRNAs, miRNAs and lncRNAs regulating low-temperature response through starch and sucrose metabolic pathways in '*Vitis amurensis* Rupr.'

evident: several miRNAs can control a single mRNA, and one miRNA can control several mRNAs. Then, from the correlation analysis of 42 key miRNAs to lncRNAs, and to mRNAs, it can be seen that miRNAs are closely related to lncRNAs and mRNAs. The evidence suggests that non-coding RNA, especially miRNA, is a key regulator of cold stress in plants [64, 65].

Certain lncRNAs function as decoys, mimicking the target DNA or RNA, to control proteins or microRNAs (miRNAs). For example, *Arabidopsis* microRNA targets mimic *IPS1* lncRNA and bait *ASCO* lncRNA [66, 67]. This demonstrates the competitive endogenous RNA (ceRNA) idea, which has gained widespread acceptance and substantial support [68, 69]. Given that the quantity of each individual miRNA is restricted, the ceRNA theory postulates that mRNA, lncRNA, pseudogenes, and other miRNA sponges share a similar miRNA binding site [69].

Conclusions

Grape cold-responsive genes were mainly enriched in starch and sucrose metabolism and were regulated by miRNAs and lncRNAs (Fig. 9), and the qRT-PCR results of most genes were consistent with the sequencing results. These results will provide basic information for further understanding of cold resistance mechanisms in grapevine in the future.

Supplementary Information

The online version contains supplementary material available at https://doi.org/10.1186/s40538-024-00611-y.

Additional file 1.

Acknowledgements
Not applicable.

Author contributions
BH C, J M, WF M and LJ M contributed to the conception of the study; WF M and SX L performed the experiment; WF L and HM G contributed to analysis and collection data; WF M performed the data analyses and wrote the manuscript; YM L, ZH M, WF L, and HM G contributed to modify paper grammar; BH C and JM helped perform the analysis with constructive discussions. All authors read and approved the final manuscript.

Funding
This research was financially supported by the Key Project of Natural Science Foundation of Gansu Province (22JR5RA831), the 2022 Modern Silk Road Cold and Drought Agricultural Science and Technology Support Project (GSLK-2022–4) and the "Innovation Star" Project of Outstanding Graduate Students in Gansu Province (2023CXZX-656).

Availability of data and materials
The data that support the findings of this study are openly available in NCBI at https://www.ncbi.nlm.nih.gov/, reference number [PRJNA1027130].

Declarations

Ethics approval and consent to participate
This manuscript is an original paper and has not been published in other journals. The authors agreed to keep the copyright rule.

Competing interests
The authors declare that they have no competing interests.

Author details
[1]College of Horticulture, Gansu Agricultural University, Lanzhou 730070, Gansu, China. [2]Shantou Forestry Research Institute, Shantou 515041, Guangdong, China.

Received: 26 April 2024 Accepted: 13 July 2024
Published online: 19 September 2024

References

1. Theine J, Holtgraewe D, Herzog K, Schwander F, Kicherer A, Hausmann L, Viehoever P, Toepfer R, Weisshaar B. Transcriptomic analysis of temporal shifts in berry development between two grapevine cultivars of the Pinot family reveals potential genes controlling ripening time. BMC Plant Biol. 2021;21(1):327.
2. Kim SA, Yun H, Soon-Young A, Han JH, Kim S, 노정호. Differential Expression Screening of Defense Related Genes in Dormant Buds of Cold-Treated Grapevines. Plant Breeding and Biotechnology. 2013; 1(1): 14–23.
3. Asgarian ZS, Karimi R, Ghabooli M, Maleki M. Biochemical changes and quality characterization of cold-stored "Sahebi" grape in response to postharvest application of GABA. Food Chem. 2022;373:131401.
4. Sreekantan L, Mathiason K, Grimplet J, Schlauch K, Dickerson JA, Fennell AY. Differential floral development and gene expression in grapevines during long and short photoperiods suggests a role for floral genes in dormancy transitioning. Plant Mol Biol. 2010;73(1–2):191–205.
5. Li P, Yu D, Gu B, Zhang H, Liu Q, Zhang J. Overexpression of the *VaERD15* gene increases cold tolerance in transgenic grapevine. Sci Hortic. 2022;293:110728.
6. Wang Z, Wong DCJ, Wang Y, Xu G, Ren C, Liu Y, Kuang Y, Fan P, Li S, Xin H, Liang Z. GRAS-domain transcription factor *PAT1* regulates jasmonic acid biosynthesis in grape cold stress response. Plant Physiol. 2021;186(3):1660–78.
7. Sanghera GS, Wani SH, Hussain W, Singh NB. Engineering cold stress tolerance in crop plants. Curr Genom. 2011;12(1):30–43.
8. Liu W, Wang Q, Zhang R, Liu M, Wang C, Liu Z, Xiang C, Lu X, Zhang X, Li X, Wang T, Gao L, Zhang W. Rootstock-scion exchanging mRNAs participate in the pathways of amino acid and fatty acid metabolism in cucumber under early chilling stress. Horticul Res. 2022;9:uhac031.
9. Rooy SSB, Ghabooli M, Salekdeh GH, Fard EM, Karimi R, Fakhrfeshani M, Gholami M. Identification of novel cold stress responsive microRNAs and their putative targets in "Sultana" grapevine (*Vitis vinifera*) using RNA deep sequencing. Acta Physiol Plant. 2023;45(1):2.
10. Nozawa M, Miura S, Nei M. Origins and evolution of MicroRNA genes in plant species. Genome Biol Evol. 2012;4(3):230–9.
11. Wang B, Wang J, Wang C, Shen W, Jia H, Zhu X, Li X. Study on expression modes and cleavage role of miR156b/c/d and its target gene Vv-SPL9 during the whole growth stage of grapevine. J Hered. 2016;107(7):626–34.
12. Kidner CA, Martienssen RA. The developmental role of microRNA in plants. Curr Opin Plant Biol. 2005;8(1):38–44.
13. Vaucheret H. Post-transcriptional small RNA pathways in plants: mechanisms and regulations. Genes Dev. 2006;20(7):759–71.
14. Rubio B, Stammitti L, Cookson SJ, Teyssier E, Gallusci P. Small RNA populations reflect the complex dialogue established between heterograft partners in grapevine. Horticult Res. 2022;9:uhab07.
15. Mallory AC, Vaucheret H. MicroRNAs: something important between the genes. Curr Opin Plant Biol. 2004;7(2):120–5.
16. Mallory AC, Bouché N. MicroRNA-directed regulation: to cleave or not to cleave(Review). Trends Plant Sci. 2008;13(7):359–67.
17. Lagos-Quintana M, Rauhut R, Lendeckel W, Tuschl T. Identification of novel genes coding for small expressed RNAs. Science. 2001;294(5543):853–8.
18. Lau NC, Lim LP, Weinstein EG, Bartel DP. An abundant class of tiny RNAs with probable regulatory roles in Caenorhabditis elegans. Science. 2001;294(5543):858–62.
19. Lee RC, Ambros V. An extensive class of small RNAs in Caenorhabditis elegans. Science. 2001;294(5543):862–4.
20. Baulcombe D. RNA silencing in plants. Nature. 2004;431(7006):356–63.
21. Voinnet O. Origin, biogenesis, and activity of plant microRNAs. Cell. 2009;136(4):669–87.
22. Bartel DP. MicroRNAs: target recognition and regulatory functions. Cell. 2009;136(2):215–33.
23. Lee RC, Feinbaum RL, Ambros V. The C elegans heterochronic gene lin-4 encodes small RNAs with antisense complementarity to lin-14. Cell. 1993;75(5):843–54.
24. Rhoades MW, Reinhart BJ, Lim LP, Burge CB, Bartel B, Bartel DP. Prediction of plant microRNA targets. Cell. 2002;110(4):513–20.
25. Pagliarani C, Vitali M, Ferrero M, Vitulo N, Incarbone M, Lovisolo C, Valle G, Schubert A. The accumulation of miRNAs differentially modulated by drought stress is affected by grafting in grapevine. Plant Physiol. 2017;173(4):2180–95.
26. Pantaleo V, Szittya G, Moxon S, Miozzi L, Moulton V, Dalmay T, Burgyan J. Identification of grapevine microRNAs and their targets using high-throughput sequencing and degradome analysis. Plant J. 2010;62(6):960–76.
27. Varkonyi-Gasic E, Gould N, Sandanayaka M, Sutherland P, MacDiarmid RM. Characterisation of microRNAs from apple (*Malus domestica* 'Royal Gala') vascular tissue and phloem sap. BMC Plant Biol. 2010;10(1):159.
28. Kullan JB, Pinto DLP, Bertolini E, Fasoli M, Zenoni S, Tornielli GB, Pezzotti M, Meyers BC, Farina L, Pe ME, Mica E. miRVine: a microRNA expression atlas of grapevine based on small RNA sequencing. BMC Genom. 2015;16(1):1–23.
29. Wang M, Sun X, Wang C, Cui L, Chen L, Zhang C, Shangguan L, Fang J. Characterization of miR061 and its target genes in grapevine responding to exogenous gibberellic acid. Funct Integr Genomics. 2017;17(5):537–49.
30. Jiu S, Leng X, Haider MS, Dong T, Guan L, Xie Z, Li X, Shangguan L, Fang J. Identification of copper (Cu) stress-responsive grapevine microRNAs and their target genes by high-throughput sequencing. Royal Soc Open Sci. 2019;6(1): 180735.
31. Mercer TR, Dinger ME, Mattick JS. Long non-coding RNAs: insights into functions. Nat Rev Genet. 2009;10(3):155–9.
32. St Laurent G, Wahlestedt C, Kapranov P. The Landscape of long noncoding RNA classification. Trends Genet. 2015;31(5):239–51.
33. Bhatia G, Sharma S, Upadhyay SK, Singh K. Long non-coding RNAs coordinate developmental transitions and other key biological processes in grapevine. Sci Rep. 2019;9(1):3552.
34. Ben Amor B, Wirth S, Merchan F, Laporte P, d'Aubenton-Carafa Y, Hirsch J, Maizel A, Mallory A, Lucas A, Deragon JM, Vaucheret H, Thermes C, Crespi M. Novel long non-protein coding RNAs involved in *Arabidopsis* differentiation and stress responses. Genome Res. 2009;19(1):57–69.
35. Zhai R, Ye S, Zhu G, Lu Y, Ye J, Yu F, Chu Q, Zhang X. Identification and integrated analysis of glyphosate stress-responsive microRNAs, lncRNAs, and mRNAs in rice using genome-wide high-throughput sequencing. BMC Genomics. 2020;21(1):238.
36. Zhang Y, Liao J, Li Z, Yu Y, Zhang J, Li Q, Qu L, Shu W, Chen Y. Genome-wide screening and functional analysis identify a large number of long noncoding RNAs involved in the sexual reproduction of rice. Genome Biol. 2014;15(12):512.
37. Li L, Eichten SR, Shimizu R, Petsch K, Yeh C-T, Wu W, Chettoor AM, Givan SA, Cole RA, Fowler JE, Evans MMS, Scanlon MJ, Yu J, Schnable PS, Timmermans MCP, Springer NM, Muehlbauer GJ. Genome-wide discovery and characterization of maize long non-coding RNAs. Genome Biol. 2014;15(2):R40.
38. Wang M, Yuan D, Tu L, Gao W, He Y, Hu H, Wang P, Liu N, Lindsey K, Zhang X. Long noncoding RNAs and their proposed functions in fibre development of cotton (*Gossypium* spp.). New Phytol. 2015;207(4):1181–97.
39. Shafiq S, Li J, Sun Q. Functions of plants long non-coding RNAs. Biochimica Et Biophysica Acta-Gene Regul Mechan. 2016;1859(1):155–62.

40. Liu J, Wang H, Chua N-H. Long noncoding RNA transcriptome of plants. Plant Biotechnol J. 2015;13(3):319–28.
41. Kim E-D, Sung S. Long noncoding RNA: unveiling hidden layer of gene regulatory networks. Trends Plant Sci. 2012;17(1):16–21.
42. Chen J, Zhong Y, Qi X. LncRNA TCONS_00021861 is functionally associated with drought tolerance in rice (*Oryza sativa* L.) via competing endogenous RNA regulation. BMC Plant Bio. 2021;21(1):410.
43. Zhang X, Dong J, Deng F, Wang W, Cheng Y, Song L, Hu M, Shen J, Xu Q, Shen F. The long non-coding RNA *lncRNA973* is involved in cotton response to salt stress. BMC Plant Biol. 2019;19(1):459.
44. Wunderlich M, Gross-Hardt R, Schoeffl F. Heat shock factor HSFB2a involved in gametophyte development of *Arabidopsis thaliana* and its expression is controlled by a heat-inducible long non-coding antisense RNA. Plant Mol Biol. 2014;85(6):541–50.
45. Liu G, Liu F, Wang Y, Liu X. A novel long noncoding RNA *CIL1* enhances cold stress tolerance in *Arabidopsis*. Plant Sci. 2022;323: 111370.
46. Zhao Z, Sun W, Guo Z, Zhang J, Yu H, Liu B. Mechanisms of lncRNA/microRNA interactions in angiogenesis. Life Sci. 2020;254: 116900.
47. Azizah1 N, Kusumaningrum1 D, Kostaman1 T, Muttaqin1 Z, Hafid1 A, Adiati1 U, Saputra1 F, Pratiwi1 N, Arrazy1 A, Koswara1 E, Manzila2 I, Gunawan3 M, Karja4 N. Seminal plasma protein profiles based on molecular weight from different bull breeds as a potential ovulatory induction factor. IOP Conference Series: Earth and Environmental Science. 2024; 012058.
48. Liu S, Wu L, Qi H, Xu M. LncRNA/circRNA-miRNA-mRNA networks regulate the development of root and shoot meristems of *Populus*. Industr Crops Product. 2019;133:333–47.
49. Wang K, Jin M, Li J, Ren Y, Li Z, Ren X, Huang C, Wan F, Qian W, Liu B. The evolution and diurnal expression patterns of photosynthetic pathway genes of the invasive alien weed, *Mikania micrantha*. J Integr Agric. 2024;23(2):590–604.
50. Zuo J, Wang Y, Zhu B, Luo Y, Wang Q, Gao L. Analysis of the coding and non-coding RNA transcriptomes in response to bell pepper chilling. Int J Mol Sci. 2018;19(7):2001.
51. Li M, Yang F, Wu X, Yan H, Liu Y. Effects of continuous cropping of sugar beet (*Beta vulgaris* L.) on its endophytic and soil bacterial community by high-throughput sequencing. Annals Microbio. 2020;70(1):1–2.
52. Langmead B, Trapnell C, Pop M, Salzberg SL. Ultrafast and memory-efficient alignment of short DNA sequences to the human genome. Genome Biol. 2009;10(3):R25–R25.
53. Ghosh S, Chakraborty J, Bhowmick S, Ghosh A, Roy S, Chatterjee R, Agarwal S, Gupta S, Chowdhury A, Datta S, Banerjee S. Protective role of a novel microRNA in liver tissues against Hepatitis C infection and its disease progression. Hep Intl. 2018;12(2):S229.
54. Peng R, Liu Y, Cai Z, Shen F, Chen J, Hou R, Zou F. Characterization and analysis of whole transcriptome of giant panda spleens: implying critical roles of long non-coding RNAs in immunity. Cell Physiol Biochem. 2018;3:1065–77.
55. Wu Q, Li B, Li Y, Liu F, Yang L, Ma Y, Zhang Y, Xu D, Li Y. Effects of PAMK on lncRNA, miRNA, and mRNA expression profiles of thymic epithelial cells. Funct Integr Genomics. 2022;22(5):849–63.
56. Yan X-M, Zhang Z, Liu J-B, Li N, Yang G-W, Luo D, Zhang Y, Yuan B, Jiang H, Zhang J-B. Genome-wide identification and analysis of long noncoding RNAs in longissimus muscle tissue from Kazakh cattle and Xinjiang brown cattle. Animal Biosci. 2021;34(11):1739–48.
57. Hasan MM, Ma F, Islam F, Sajid M, Prodhan ZH, Li F, Shen H, Chen Y, Wang X. Comparative transcriptomic analysis of biological process and key pathway in three cotton (*Gossypium* spp.) species under drought stress. Int J Mol Sci. 2019;20(9):2076.
58. Li K, Wu G, Li M, Ma M, Du J, Sun M, Sun X, Qing L. Transcriptome analysis of *Nicotiana* benthamiana infected by Tobacco curly shoot virus(Article). Virol J. 2018;1:1–15.
59. Zuo J, Wang Y, Zhu B, Luo Y, Wang Q, Gao L. sRNAome and transcriptome analysis provide insight into chilling response of cowpea pods. Gene. 2018;671:142–51.
60. Reinhart BJ, Weinstein EG, Rhoades MW, Bartel B, Bartel DP. MicroRNAs in plants. Genes Dev. 2002;16(13):1616–26.
61. Young MD, Wakefield MJ, Smyth GK, Oshlack A. Gene ontology analysis for RNA-seq: accounting for selection bias. Genome Biol. 2010;11(2):R14.
62. Ashburner M, Ball CA, Blake JA, Botstein D, Butler H, Cherry JM, Davis AP, Dolinski K, Dwight SS, Eppig JT, Harris MA, Hill DP, Issel-Tarver L, Kasarskis A, Lewis S, Matese JC, Richardson JE, Ringwald M, Rubin GM, Sherlock G. Gene ontology: tool for the unification of biology. The gene ontology consortium. Nat Genet. 2000;25(1):25–9.
63. Sun X, Fan G, Su L, Wang W, Liang Z, Li S, Xin H. Identification of cold-inducible microRNAs in grapevine. Front Plant Sci. 2015;6(8):595.
64. Dong C-H, Pei H. Over-expression of *miR397* improves plant tolerance to cold stress in *Arabidopsis thaliana*. J Plant Biol. 2014;57(4):209–17.
65. Wang J, Meng X, Dobrovolskaya OB, Orlov YL, Chen M. Non-coding RNAs and their roles in stress response in plants. Geno Proteom Bioinformat. 2017;15(5):301–12.
66. Bardou F, Ariel F, Simpson CG, Romero-Barrios N, Laporte P, Balzergue S, Brown JWS, Crespi M. Long noncoding RNA modulates alternative splicing regulators in *Arabidopsis*. Dev Cell. 2014;30(2):166–76.
67. Franco-Zorrilla JM, Valli A, Todesco M, Mateos I, Puga MI, Rubio-Somoza I, Leyva A, Weigel D, Garcia JA, Paz-Ares J. Target mimicry provides a new mechanism for regulation of microRNA activity. Nat Genet. 2007;39(8):1033–7.
68. Wierzbicki AT, Haag JR, Pikaard CS. Noncoding transcription by RNA polymerase Pol IVb/Pol V mediates transcriptional silencing of overlapping and adjacent genes. Cell. 2008;135(4):635–48.
69. Zhang Y-C, Chen Y-Q. Long noncoding RNAs: New regulators in plant development. Biochem Biophys Res Commun. 2013;436(2):111–4.

Publisher's Note